

# Investigating toxicity and antimicrobial properties of silver nanoparticles in *Escherichia coli* and *Drosophila melanogaster*

Abhijeet Ghosh, Tobie Hendricks

Biomedical STEM Academy, Walton High School, Marietta, Georgia

## SUMMARY

Silver nanoparticles (AgNPs) hold significant promise as an antimicrobial agent and in various biomedical applications. However, AgNPs have toxic health effects linked to their structural properties, such as surface coating, concentration, and size. These properties, when studied in isolation and in combination, must be examined to determine the optimal configuration that minimizes toxicity and maximizes the efficacy of AgNPs for medical applications. This study investigated the toxicity of AgNPs with varying sizes, concentrations, and surface coatings. The toxic effects of citrate-capped and plant-based AgNPs were studied on two model organisms: a species of bacteria, *Escherichia coli* (*E. coli*); and the fruit fly, *Drosophila melanogaster* (*D. melanogaster*). The research was guided by three hypotheses: AgNPs would be toxic to *E. coli* and *D. melanogaster*, although toxicity would decrease with increasing nanoparticle size and decreasing concentration; *D. melanogaster* would be more resilient to AgNPs than *E. coli*; and plant-based AgNPs would have higher toxicity to *E. coli* and lower toxicity to *D. melanogaster* than citrate-capped AgNPs. The results showed that smaller-sized citrate-capped AgNPs were highly toxic to *E. coli* even at low concentrations (2 mg/L), while being safer for *D. melanogaster*. It was also found that plant-based AgNPs were more toxic to *E. coli*. Overall, the findings suggest that AgNP toxicity can be modulated by adjusting their size, surface coating, and concentration. These findings highlight the potential of AgNPs in medical applications, paving the way for innovative antimicrobial and therapeutic products.

## INTRODUCTION

Medicinal use of silver expanded significantly during the 18th and 19th centuries, when surgeons started using silver for its antibacterial properties for sutures in wound closures and treatment for infections. However, its use declined after the discovery of penicillin in 1928, which made antibiotics a more convenient alternative (1,2). By the mid-20th century, silver had largely fallen out of favor in mainstream medicine (3). The emergence of antibiotic-resistant bacteria in the late 20<sup>th</sup> and early 21<sup>st</sup> century rekindled interest in silver's antimicrobial properties (2,3). Silver's broad-spectrum efficacy against bacteria, viruses, and fungi, and its ability to disrupt biofilms, made it an attractive alternative to traditional

antibiotics (1,4,5). Recently, silver nanoparticles (AgNPs) and related products have emerged as promising alternatives in medicine due to their antimicrobial properties (6-8). Silver nanoparticles are solid masses of silver with a diameter of 1–100 nm, and they are often coated with another molecule, called the capping agent, to improve biological activity and stability (6-9).

Studies have consistently shown that, because of their large surface area, AgNPs can penetrate bacterial cell walls and animal cell membranes. This leads to the denaturation of deoxyribonucleic acid (DNA), lysosomes, and ribosomes, generating reactive oxygen species that ultimately cause cell death (6-8).

While AgNPs have proven effective in many medical applications, concerns about environmental impact and toxicity have emerged. Silver is known to be toxic to humans, causing symptoms like liver and kidney failure (9). Silver also causes significant destruction to the environment and ecosystems, especially to aquatic ecosystems (10). Nevertheless, the toxicity of AgNPs is variable and can be modified by varying their physicochemical properties, such as size, surface coating, shape, and concentration, among others (11).

Studies are needed to understand the toxicology of AgNPs so that safe AgNPs can be designed to maximize silver's health benefits while minimizing the risks. Combining silver with other antimicrobial agents, optimizing nanoparticle design, and exploring the use of silver in conjunction with other treatments are under active investigation (11). This study investigated the effect of varying the size, concentration, and surface coating of AgNPs on AgNP toxicity in *Escherichia coli* (bacteria) and *Drosophila melanogaster* (fruit flies). The purpose of this study was to increase the understanding of AgNPs' toxic effects, how the toxic effects can be modified by altering AgNPs' properties, and how these effects compare between *E. coli* and *D. melanogaster*. This knowledge is expected to inform research on engineering safe AgNPs to reduce toxicity while enhancing their utilization for antimicrobial and other therapeutic applications.

There are three main methods for nanoparticle synthesis: physical, chemical, and biological (12). Physical methods involve breaking down silver metal into nanoparticles (9,12). Chemical methods involve reducing silver ions into nanoparticles using reducing agents and stabilizing them with capping agents, where the reducing agent reacts with Ag<sup>+</sup> to form metallic silver and the capping agent binds to the outside of the AgNPs to stabilize them (9). Biological methods replace expensive and/or toxic chemical reducing agents with natural alternatives (9,12).

In recent years, biological synthesis methods of AgNPs, using bacteria, fungi, and plant extracts, have attracted increasing attention due to their simplicity, cost-effectiveness, and eco-friendly nature (7,13). In plant-based synthesis, organic molecules (proteins, enzymes, sugars) and phytochemicals found in plant extracts (flavonoids, polyphenols, terpenoids, flavonoids, alkaloids, and aldehydes) aid in reducing and coating silver ions into AgNPs (13,14). Plant-based synthesis has many advantages over conventional physical and chemical methods: it uses less energy (heat), involves eco-friendly chemicals or natural ingredients, and is easier to regulate (7). For this study, a broth derived from *Murraya koenigii* (commonly known as curry leaf) was used for the plant-based synthesis of AgNPs, serving as both the reducing and capping agent. *Murraya koenigii* (*M. koenigii*) is known for its antioxidant, anti-inflammatory, and antibacterial properties, some of which are imparted to the AgNPs through the adsorption of the plant's organic compounds onto the AgNPs' surface (15).

This study hypothesized that: (i) AgNPs would be toxic to both bacteria (*Escherichia coli*) and fruit flies (*Drosophila melanogaster*), though toxicity would decrease as the size of the AgNPs increased and as the concentration of AgNPs decreased; (ii) *Drosophila melanogaster* (*D. melanogaster*) would be more resilient to AgNPs than *Escherichia coli* (*E. coli*); (iii) plant-based AgNPs would have higher toxicity than citrate-capped AgNPs to *E. coli* due to the antimicrobial effects of *M. koenigii*, and lower toxicity to *D. melanogaster* due to antioxidant properties. Some hypotheses were refuted and others corroborated by the study's findings: more concentrated AgNPs were more toxic in all organisms; smaller AgNPs were less toxic in *D. melanogaster* and more toxic in *E. coli* than larger NPs; and the plant-based NPs were much more toxic in both organisms. The results underscore the importance of further investigating AgNPs' size, shape, coating, and other properties, independently and in combination, to identify the optimal properties that enhance their antibacterial effects while minimizing associated risks. Once the optimal properties are identified, AgNPs may be used in conjunction with or as a replacement for antibiotics with nearly no risk of resistance, helping combat antibiotic resistance and decrease antibiotic use.

## RESULTS

This study aimed to investigate the impact of AgNPs' size, concentration, and surface coating on antimicrobial properties in *E. coli* and toxicity *in vivo* in *D. melanogaster*, helping find the optimal properties to reduce AgNPs' off-target effects while maintaining strong antibacterial properties.

### Characterizing the AgNPs by Size and Concentration

To measure AgNPs' particle size and concentration, spectrophotometry was performed. Larger AgNPs absorb larger wavelengths of light compared to smaller AgNPs, and concentration linearly correlates with absorbance, hence relating the absorption spectra to size/concentration (14-16). Citrate-capped nanoparticles were produced in sizes ranging from 39.6 nm to 75.1 nm and in concentrations ranging from 2 mg/L to 161 mg/L (Table 1). Plant-based nanoparticles (made from *M. koenigii* extract) were produced in sizes ranging from 61.3 nm to 84.9 nm and in concentrations ranging from 8 mg/L to 42 mg/L (Table 1). The wide range of sizes synthesized

allowed for testing on both mid-size and large AgNPs, leading to more robust data; the variety of concentrations similarly allowed for measuring both toxic effects at overdoses and antibacterial effects at minute concentrations.

### Dose and Size Dependent Antibacterial Effects of AgNPs in *E. coli*

In order to understand the antibacterial effects of different-sized AgNPs, *E. coli* was exposed to AgNP solutions with two types of surface coatings (citrate and plant-based) and of various sizes (40 to 90 nm). The citrate-capped AgNP solutions significantly reduced the number of bacterial colonies, with an average of 51.7% colony growth compared to the control (Figure 1; SD = 13.3,  $p < 0.01$  in one-way ANOVA with post-hoc Dunnett's test). The plant-based AgNPs were much more toxic than the citrate-coated AgNPs, with an average of 19.1% colony growth (Figure 1, SD = 9.8,  $p < 0.01$  in one-way ANOVA with post-hoc Dunnett's test). In terms of concentration, for citrate-capped AgNPs, the 20 mg/L AgNPs reduced colony growth by 11.8% compared to 2 mg/L AgNPs (two-tailed  $t$ -test,  $p < 0.01$ ), demonstrating a dose-response effect (Figure 2). For plant-based NPs, 20 mg/L AgNPs had an average of 12.6% more colony reduction than 2 mg/L AgNPs (two-tailed  $t$ -test,  $p < 0.01$ ), again demonstrating a dose-dependent response (Figure 2). Finally, the smaller citrate-capped nanoparticles also demonstrated greater toxicity compared to larger NPs (Figure 3A). The inverse relationship between size and toxicity was also observed in plant-based AgNPs (Figure 3B).

### Dose and Size Dependent Toxicity of AgNPs in *D. melanogaster*

*D. melanogaster* cultures were allowed to replicate while exposed to AgNPs. Larval growth was used as the indicator of health. The smaller citrate-capped AgNPs were relatively non-toxic to *D. melanogaster*, indicating possible safe use of AgNPs in other complex organisms (Figure 4A). The 42 nm AgNPs at 20 mg/L increased larvae growth by 29%, suggesting they were beneficial to *D. melanogaster*. Additionally, the average number of larvae for AgNPs under 60 nm was 98.5% of the number of larvae for the control condition, indicating nearly no difference in growth from the control (Figure 4). For all citrate-capped AgNPs, there was no statistical difference between exposed *D. melanogaster* and controls, indicating that the AgNPs had little side effects/toxicity (Figure 1). The higher concentration of 40 mg/L AgNPs reduced growth, on average, by 18.4% more than the lower concentration of 20 mg/L AgNPs, suggesting that the beneficial effects of AgNPs in *D. melanogaster* are lost at higher AgNP concentrations (Figure 4). The plant-based AgNPs were more toxic to *D. melanogaster* than the citrate-capped AgNPs, with an average of 20.1% (SD = 31.1) larval growth compared to the control. There was also an inverse relationship between size and toxicity with plant-based AgNPs, which was similar to the relationship observed in *E. coli* but contrary to the relationships observed with the citrate AgNPs in *D. melanogaster*.

## DISCUSSION

The objective of this study was to observe trends in antibacterial effects and toxicity of AgNPs while varying their physicochemical properties, including size, concentration, and

ID	AgNO <sub>3</sub> Conc. (mM)	AgNO <sub>3</sub> Volume (mL)	Citrate Conc. (mM)	Citrate Volume (mL)	Heating Time (mins)	Broth Volume (mL)	AgNP Size (nm)	AgNP Conc. (mg/L)	
Citrate-Capped AgNPs	1	1.0	15	10	1.0	5	NA	39.6	3.1
	2	1.0	15	10	2.0	3	NA	50.1	6.1
	3	1.0	15	10	0.4	5	NA	52.1	3.2
	4	1.0	15	1	2.0	7	NA	50.1	1.6
	5	1.0	15	5	0.6	20	NA	57.8	13.5
	6	1.0	15	5	1.0	7	NA	53.1	29.2
	7	1.0	15	10	0.6	10	NA	45.7	5.5
	8	5.0	15	10	1.0	2	NA	55.0	7.0
	9	1.0	15	20	0.8	4	NA	40.9	3.0
	10	1.0	15	10	2.0	15	NA	50.1	102
	11	2.0	15	10	1.4	15	NA	67.0	51.0
	12	1.0	15	20	1.4	3	NA	53.1	6.8
	13	1.0	15	40	0.4	5	NA	43.4	1.6
	14	1.0	15	10	0.8	20	NA	59.6	87.2
	15	2.0	15	15	1.0	4	NA	57.8	8.4
	16	2.0	15	100	1.0	1.5	NA	57.8	30.3
	17	2.0	15	100	1.0	1.5	NA	57.8	15.7
	18	2.0	15	10	2.0	25	NA	45.7	106
	19	3.0	15	10	3.0	25	NA	45.7	161
	20	2.0	15	100	1.0	15	NA	42.1	105
	21	3.0	15	100	1.0	1.5	NA	55.0	13.3
	22	1.0	15	100	1.0	3.5	NA	63.0	34.9
	23	0.5	15	100	1.0	2.5	NA	58.7	17.8
	24	4.0	18	100	1.0	15	NA	45.7	161
	25	4.0	18	100	2.0	2	NA	54.1	0.6
	26	4.0	18	15	2.0	7	NA	126	32.0
	27	3.0	18	15	2.0	7	NA	58.7	21.5
	28	1.0	17	10	1.6	15	NA	63.8	56.6
	29	1.0	16	10	1.7	15	NA	47.9	34.6
	30	1.0	17	100	1.0	4	NA	56.9	12.8
	31	1.0	17	10	1.0	20	NA	75.1	48.0
	32	1.5	17	100	1.4	15	NA	56.9	62.8
Plant-Based AgNPs	33	1.0	17	NA	NA	NA	0.86	70.8	21.6
	34	1.0	18	NA	NA	NA	0.09	61.3	7.5
	35	1.0	17	NA	NA	NA	0.57	NR	NR
	36	1.0	17	NA	NA	NA	0.17	NR	NR
	37	1.0	17	NA	NA	NA	0.28	NR	NR
	38	1.0	17	NA	NA	NA	0.11	NR	NR
	39	1.0	17	NA	NA	NA	0.09	NR	NR
	40	1.0	17	NA	NA	NA	0.09	76.5	11.8
	41	1.0	17	NA	NA	NA	0.11	76.5	15.5
	42	1.0	17	NA	NA	NA	0.28	81.7	32.7
	43	1.0	17	NA	NA	NA	0.17	79.1	19.9
	44	1.0	17	NA	NA	NA	0.41	84.9	41.6

**Table 1. Summary of the AgNPs synthesized.** The volumes and concentrations of reagents used to generate citrate-capped and plant-based AgNPs and the resulting sizes and concentrations of synthesized AgNPs. NR refers to not read (not characterized in the spectrometer), as some solutions failed to synthesize correctly and did not need to be characterized. NA; not applicable. Curry leaf broth was not used in synthesizing citrate-capped AgNPs. Likewise, sodium citrate and heating were not used in plant-based AgNP synthesis.

surface coating. This study found that, as AgNP concentrations increased, toxicity to *E. coli* and *D. melanogaster* increased. Additionally, the *E. coli* results showed an inverse relationship between AgNP size and toxicity for all concentrations and surface coatings. On the other hand, *D. melanogaster* was less affected by the AgNPs overall than *E. coli*, even though the concentration was higher, supporting the hypothesis that *D. melanogaster* is more resilient to AgNPs than *E. coli*.

Unexpectedly, the smaller citrate-capped AgNPs were less toxic than the larger AgNPs in *D. melanogaster*, unlike in *E. coli*. For example, the 42 nm citrate-capped nanoparticles at 20 mg/L promoted larval growth, rather than hindering it. In terms of plant-based AgNPs, they were much more toxic than citrate-capped AgNPs in both organisms. This fails to support the hypothesis that plant-based NPs would be less toxic to *D. melanogaster*. Finally, there was an inverse

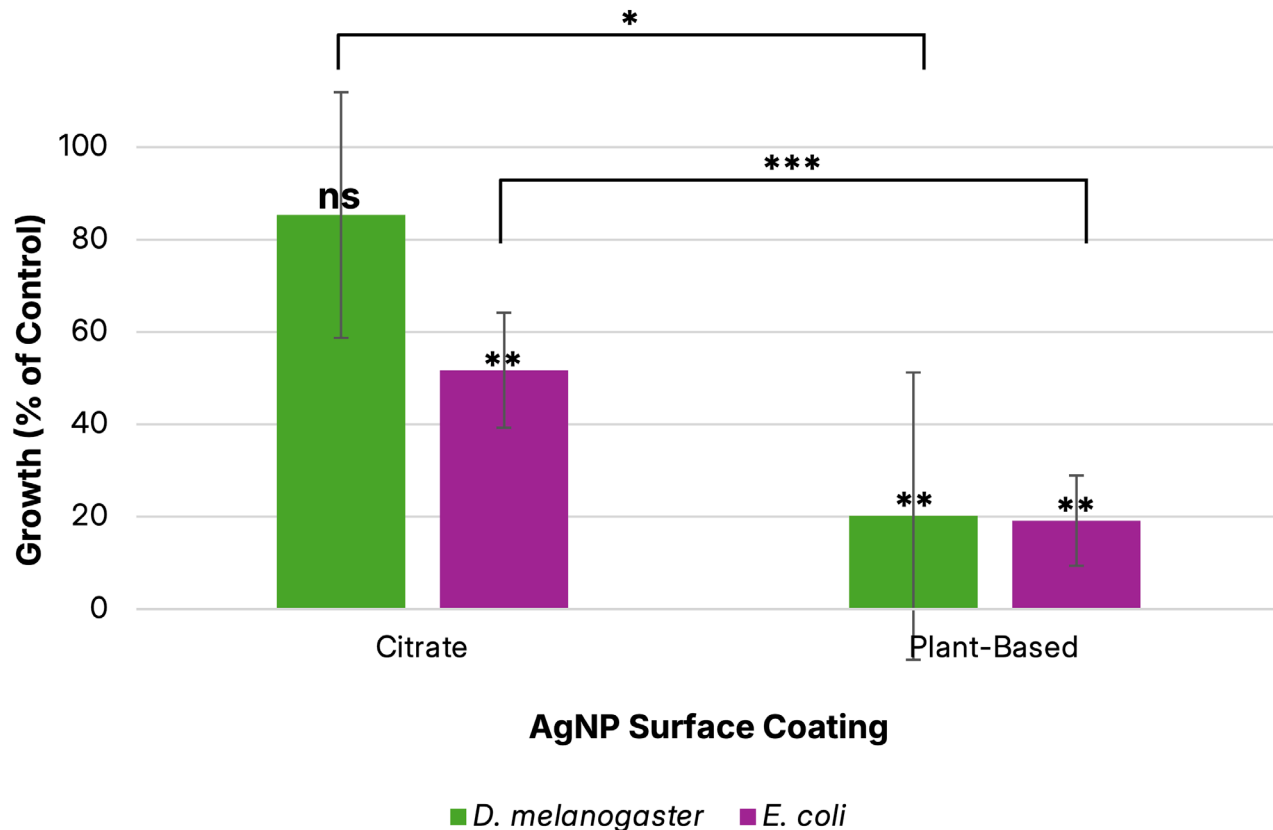


**Figure 1. *E. coli* growth and *D. melanogaster* larval growth were dependent on the surface coating of silver nanoparticles (AgNPs).** Average *E. coli* growth (purple bars) and larval growth (green bars) when exposed to citrate-capped and plant-based AgNPs. Error bars denote the standard deviation. All samples per group were averaged together to compare one variable: *D. melanogaster* citrate had 6 replicates; *D. melanogaster* plant-based had 3 replicates; *E. coli* citrate had 27 replicates; *E. coli* plant-based had 18 replicates. One-way ANOVA ( $p < 0.001$ ) with Dunnett's post-hoc test compared all samples to the control; two-tailed *t*-tests compared the results between surface coatings within each species. Asterisks represent  $p$  values: ns is no significance, \* represents  $p < 0.05$ , \*\* represents  $p < 0.01$ , \*\*\* represents  $p < 0.001$ .

correlation between size and toxicity for plant-based AgNPs in *D. melanogaster*, contrary to the citrate AgNPs.

Existing literature is still short on the mechanism behind the toxicity of AgNPs; however, several chemical pathways have been observed. The primary proposed mechanism is that AgNPs bind through cell membranes (and bacterial cell walls), thereby triggering cell membrane denaturation via the release of Ag<sup>+</sup> ions. Once AgNPs enter cells, released Ag<sup>+</sup> ions denature DNA, organelles, and proteins due to silver's strong reduction potential. Such denaturation leads to oxidative stress, resulting in cell lysis (6,9). In complex organisms, the mechanism remains the same, and AgNPs are able to penetrate into tissues via absorption through epithelia (GI tract lining, skin, lungs, etc.) and circulation in the bloodstream (17).

Both organisms experienced greater toxicity at higher AgNP concentrations, which is in agreement with previous studies (9,18,19). The dose-response effect of AgNPs is primarily due to the availability of silver ions at different concentrations (9,18). At lower AgNP concentrations, fewer silver ions are released, resulting in reduced bacterial damage (19). However, at higher AgNP concentrations, silver ion concentration increases, leading to a strong antibacterial and toxic effect (19). AgNPs induce oxidative stress by generating reactive oxygen species (ROS) within cells,

including superoxide anions (O<sub>2</sub><sup>-</sup>) and hydrogen peroxide (H<sub>2</sub>O<sub>2</sub>) (20-22). ROS damage cell membranes, proteins, and DNA, ultimately resulting in cell death. The production of ROS is directly related to the concentration of AgNPs, with higher concentrations resulting in more ROS production (22,23).

The relation between AgNP size and toxicity was not as simple. In *E. coli*, toxicity increased as the size decreased, regardless of concentration and surface coating. The inverse relationship between AgNP size and toxicity is likely due to the increase in the surface area to volume ratio of silver with decreasing AgNP size. The larger the surface area to volume ratio, the faster the dissolution of silver ions from the AgNP, resulting in increased availability and distribution of the silver ions, and a stronger antimicrobial effect (24). Additionally, smaller nanoparticles are more likely to induce oxidative stress by producing higher levels of ROS (21). For example, smaller AgNPs induce significantly higher ROS production in *E. coli* compared to larger NPs, contributing to the greater toxicity of smaller particles (21). In line with this study's findings, a prior study by Kong et al. found that smaller AgNPs have twofold higher toxicity (enzymatic activity) than larger AgNPs (25).

On the other hand, in *D. melanogaster*, toxicity decreased as size decreased for citrate-capped AgNPs, while toxicity increased as size decreased for plant-based NPs. Though

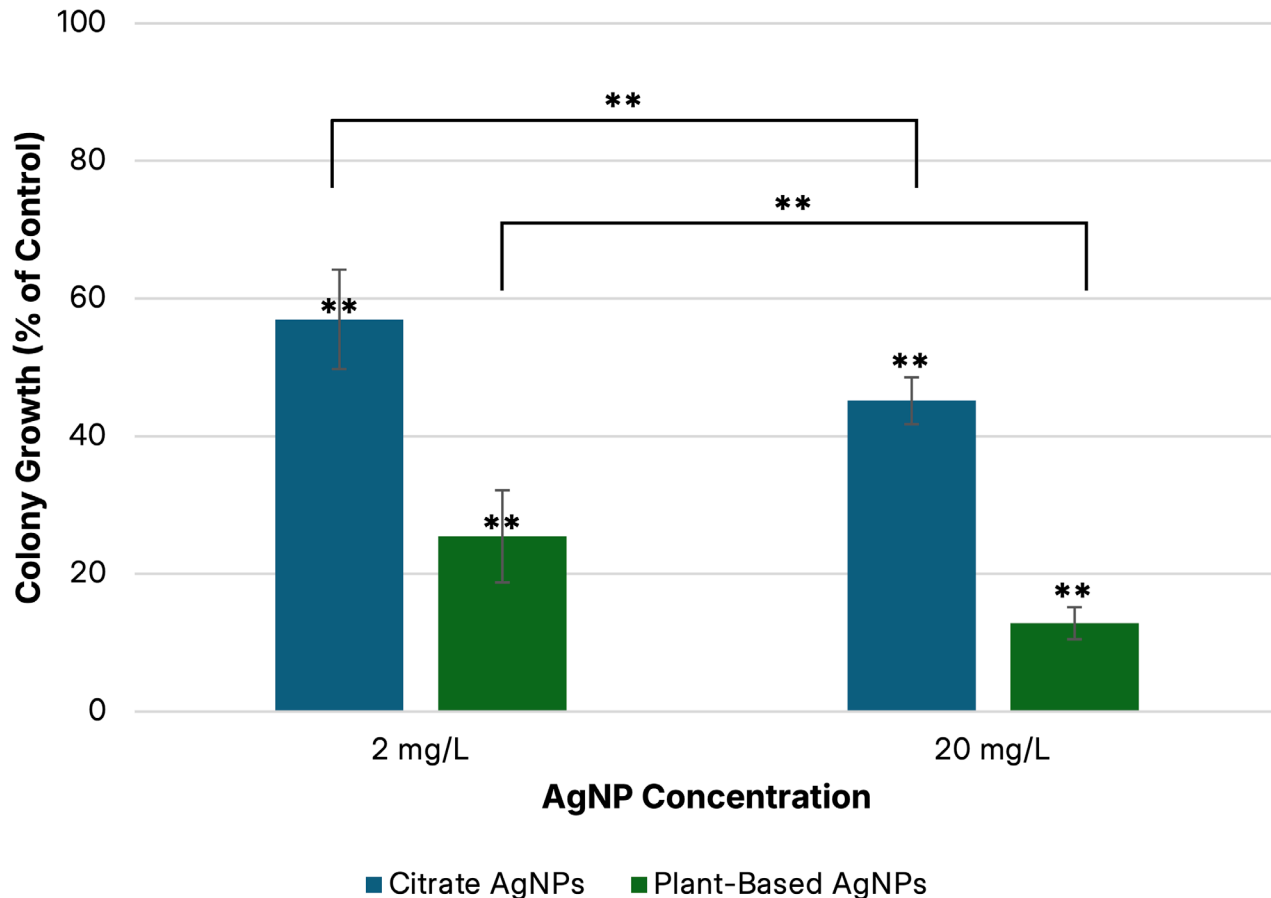


**Figure 2. *E. coli* growth was dependent on the concentration of AgNPs.** Average *E. coli* growth when exposed to 2 mg/L and 20 mg/L AgNPs (n=9–15), for both citrate-capped AgNPs (blue bars) and plant-based AgNPs (green bars). Error bars denote standard deviation. One-way ANOVA ( $p < 0.001$ ) with Dunnett's post-hoc test compared all samples to control; two-tailed  $t$ -tests compared the results of different concentrations within each type of AgNP. Asterisks represent  $p$  values: ns is no significance, \* represents  $p < 0.05$ , \*\* represents  $p < 0.01$ , \*\*\* represents  $p < 0.001$ .

this result diverges from some existing literature on other organisms, multiple possible explanations make this result plausible for *D. melanogaster* (14,24,26,27). One explanation is that there is a notable correlation between AgNP stability and toxicity, as AgNPs that readily aggregate with themselves or bind to other surfaces quickly lose toxicity. Larger AgNPs are more resistant to aggregation and adhesion due to their larger mass, so they can end up being more toxic in the long term (26). This explanation is consistent with this study's results, as *D. melanogaster* testing was more long-term than *E. coli* testing (7 days vs. 1 day), so the aggregation of the smaller nanoparticles would be a greater factor in the *D. melanogaster* trials than the *E. coli* trials. Secondly, research has shown that a particular size of nanoparticle has maximum, or peak, toxicity for complex organisms, and nanoparticles smaller and larger than the peak size are less toxic. The nanoparticles of the peak size are more likely to become trapped in various body tissues, such as the intestines, which leads to much greater toxicity than smaller nanoparticles that are readily excreted or metabolized (28). The NPs larger than the peak size are unable to be absorbed into tissues and are filtered by epithelium, like the skin or GI tract. This peak size differs for each organism and surface coating, depending on how strongly the coating bonds to

tissues and other molecules (16,24). In this study, the peak size appeared to be 70–80 nm, as the larger plant-based nanoparticles (85 nm) had reduced toxicity compared to the smaller plant-based nanoparticles, though this estimate is not exact due to the differing properties between plant-based and citrate-capped AgNPs.

Plant-based AgNPs were more toxic than citrate-capped NPs in both *E. coli* and *D. melanogaster*, likely due to the insecticidal and antibiotic compounds in *M. koenigii* that were transferred to the AgNPs (29). *M. koenigii* has been shown to have antioxidant, anti-inflammatory, and antibacterial effects; some of these properties were carried over to the AgNPs through the coating molecules (15). Additionally, these molecules may enhance the AgNPs' interactions with cells by improving cell membrane penetration and facilitating specific interactions with surface proteins, thereby increasing their toxicity (7). Yadav and Preet showed that plant-derived AgNPs induced higher levels of ROS production and greater disruption of cell membranes compared to chemically synthesized nanoparticles (30). Additionally, phytochemicals present in the plant extract may enhance the stability of the nanoparticles, improving their interaction with bacterial cell walls and leading to more effective antibacterial action (30).

This study faced some limitations. For example, the

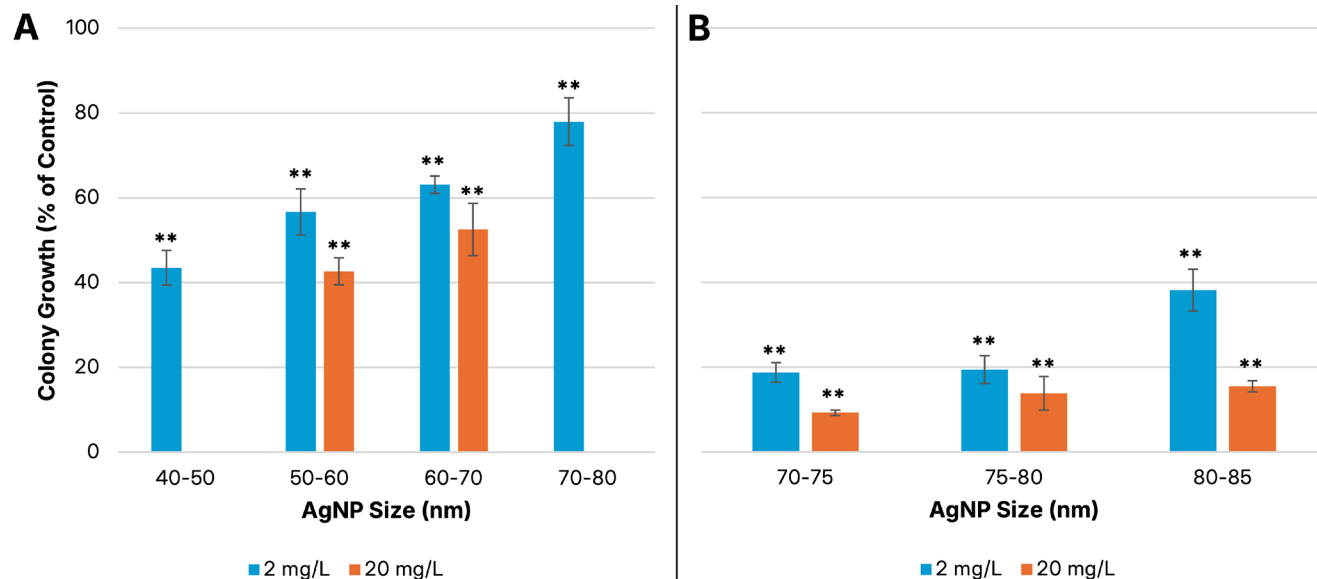


**Figure 3. *E. coli* growth was dependent on the size of AgNPs.** A) Average *E. coli* growth following exposure to different sizes of citrate-coated AgNPs (n=3–9) at both low concentrations (blue bars, 2 mg/L) and moderate concentrations (orange bars, 20 mg/L). AgNPs could not be synthesized at 20 mg/L for sizes of 40–50 nm and 70–80 nm. B) Average *E. coli* growth following exposure to different sizes of plant-based AgNPs (n=3) at both concentrations. Error bars denote standard deviation. One-way ANOVA ( $p < 0.001$ ) with Dunnett's post-hoc test compared all samples to the control. Asterisks represent  $p$  values: ns is no significance, \* represents  $p < 0.05$ , \*\* represents  $p < 0.01$ , \*\*\* represents  $p < 0.001$ .

AgNP solutions were used directly after synthesis without washing/centrifuging. Instead, they could have been washed (centrifuged and redispersed in water or 1 mM sodium citrate) to remove any excess reagents that might not have reacted. This would have reduced the effect of the confounding toxicity of unreacted reagents, such as excess AgNO<sub>3</sub> or excess curry leaf broth. Nevertheless, mass-based calculations show that the amount of remaining AgNO<sub>3</sub> was negligible after synthesis, and most other reagents (like sodium citrate) are relatively non-toxic.

Another limitation was that the *D. melanogaster* testing was performed with one replicate due to limited access to laboratory resources and time. While the results provide insight into the effects of the synthesized nanoparticles in complex organisms, additional replicates are necessary to assess reproducibility and statistical reliability. Future studies should aim to repeat these experiments under the same conditions to validate the observed trends and strengthen the conclusions drawn. Plant-based AgNPs should have been tested at 2 mg/L or 10 mg/L in *D. melanogaster* due to their extremely high toxicity at 20 mg/L. The lower concentration would also provide a direct comparison to the *E. coli* testing results. Such high toxicity in *D. melanogaster* was not expected; hence why low-concentration trials were not conducted. However, in the trials with citrate-capped AgNPs, the assumption on low-concentration toxicity held true, as even the moderate to high concentrations had minimal to moderate toxicity, providing valuable results and conclusions.

In summary, the results showed that smaller-sized citrate-capped AgNPs were highly toxic to *E. coli* even in low concentrations (2 mg/L), affirming the antibacterial effects of AgNPs, while being safer for *D. melanogaster* (a complex organism). It was also found that plant-based AgNPs were more toxic against *E. coli* due to the bioactive molecules in the *M. koenigii* that enhance bacterial cell wall interaction

and their antibacterial efficacy. Overall, the findings suggest that the toxicity of AgNPs can be modified by altering their size and structuring them into composite formations. A noteworthy finding is the high antibacterial effects but low toxicity in *D. melanogaster* of smaller, citrate-capped AgNPs. These AgNPs, in fact, promoted growth in *D. melanogaster*, likely because they were able to target pathogens in the environment, but they would not accumulate and damage tissues in *D. melanogaster* due to their small size. These findings provide valuable insights into harnessing AgNPs for their antibacterial and therapeutic properties, and this knowledge could further pave the way to the development of innovative antibiotic alternatives and medications.

## MATERIALS AND METHODS

The study was designed as a two-phase process. The first phase involved the synthesis of AgNPs and characterization by size and concentration. Two types of synthesis methods were used: chemical and plant-based synthesis. The second phase involved measuring the toxicity of AgNPs of varying sizes, concentrations, and surface coatings in *D. melanogaster* and *E. coli*.

### Phase I: Synthesis and Characterization of AgNPs

#### Chemical Synthesis: Citrate-capped AgNPs

Chemical synthesis is currently the most common method of synthesizing AgNPs (9,31). In this process, silver (Ag<sup>+</sup>) ions are reduced to AgNPs in the presence of a reducing agent, such as sodium citrate, sodium borohydride, or polyvinyl alcohol. They are then coated by a capping agent, which can either be the reducing agent or a variety of different coating molecules (31).

In this study, the procedure for synthesizing AgNPs was self-designed and based on the Turkevich method, which involves using a boiling sodium citrate solution to reduce

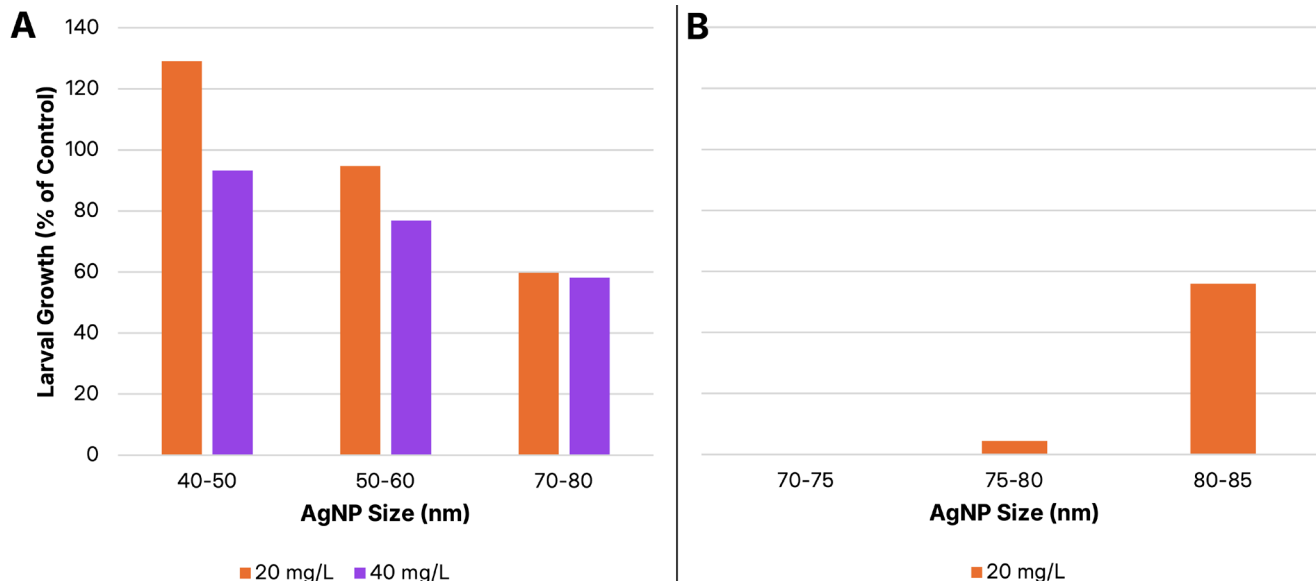


**Figure 4. *D. melanogaster* larval growth was dependent on the size and concentration of AgNPs.** A) Average larval growth following exposure to different sizes of citrate-coated AgNPs (n=1). AgNPs were administered at moderate doses of 20 mg/L (orange bars) and higher doses of 40 mg/L (purple bars) to find risks associated with overdosage. B) Average larval growth following exposure to different sizes of plant-based AgNPs (n=1). No statistical tests were performed due to low sample size.

various metal ions into nanoparticles (NPs) and form a coating around the NPs that stabilizes them (31-33). Trisodium citrate was used as both the reducing and capping agent, as sodium citrate is less toxic and safer than other reducing agents like sodium borohydride (33). To alter the size of the NPs, the concentration of both reagents (silver nitrate and sodium citrate) could be modified. Additionally, changing the amount of time the solution was held at a boil would change the size. The first step in chemical synthesis is the preparation of stock solutions. Trisodium citrate dihydrate crystals (Innovating Science), silver nitrate stock solution (0.1 M, Innovating Science), and distilled water were used to synthesize citrate-capped AgNPs. Sodium citrate was dissolved in distilled water to form 0.1 M stock solutions. During later steps of the synthesis, silver nitrate and sodium citrate stock solutions were diluted further to varying concentrations using distilled water (Figure 5A, step 1).

The next step involved the reaction of  $\text{Ag}^+$  ions with citrate. In this step, 15–18 mL of diluted silver nitrate solution was brought to a boil (Table 1; Figure 5A, step 2). 0.4–3 mL of diluted trisodium citrate solution (Table 1) was added dropwise to the silver nitrate solution over a minute (Figure 5A, step 3). During this time, the citrate ions reduced  $\text{Ag}^+$  ions into  $\text{Ag}^0$  atoms, which then aggregated and were stabilized by the remaining citrate molecules, forming citrate-capped AgNPs. After waiting 1.5–20 minutes, the solution was rapidly cooled (Figure 5A, step 4; Table 1). By this point, the solution had turned yellow and/or cloudy, signifying that AgNPs had formed. The solution was then stored in the dark to prevent light-based degradation of the AgNPs.

#### Plant-Based Synthesis: *M. koenigii*-capped AgNPs

This study used *M. koenigii* (curry leaf) extract to synthesize AgNPs. The major carbazole alkaloids and terpenoids in the curry leaf extract reduced and coated the AgNPs (14). The first step in plant-based synthesis was the

preparation of *M. koenigii* broth. Five grams of fresh leaves were collected from a *M. koenigii* plant and used within 12 hours. They were washed twice in distilled water and minced into 1 mm-thick strips (Figure 5B, step 1). The minced leaves were soaked in 37.5 mL of distilled water and brought to a boil (Figure 5B, step 2). 100°C was maintained for 3 minutes, and then the broth was allowed to cool. The leaves were filtered out, leaving approximately 25 mL of curry leaf broth (Figure 5B, step 3). The broth was used within six hours, and excess broth was disposed of.

To synthesize AgNPs, a small variable amount of curry leaf broth was added to 1 mM silver nitrate solution at room temperature (Figure 5B, steps 4 and 5). This solution was stored for a minimum of 24 hours in the dark to ensure that nanoparticles had reached an equilibrium size and concentration (Figure 5B, step 6).

#### Characterization of Synthesized AgNPs: UV-Visible Spectrometry

UV-visible spectrometry was used to characterize AgNPs by size and concentration. AgNPs absorb light around 350–450 nm, and larger NPs absorb longer wavelengths of light. The size of each AgNP sample was calculated using the wavelength where maximum absorption occurred (34). For each AgNP size, the picomolar concentration was then determined using the Molar Excitation Coefficient ( $\epsilon$ ) at that size of NP, the peak absorbance, and the Beer-Lambert law (34). For concentration in mg/L, the mass of one silver nanoparticle was multiplied by the number of particles (molar concentration multiplied by Avogadro's number) (Table 1) (35).

A Cary 5000 UV-Vis-NIR Spectrophotometer was used for this research. The spectrometer was first calibrated with a baseline correction of distilled water, then all AgNP suspensions were measured. Absorption measurements were taken from 375 to 475 nm (Figure 7). Sometimes, the

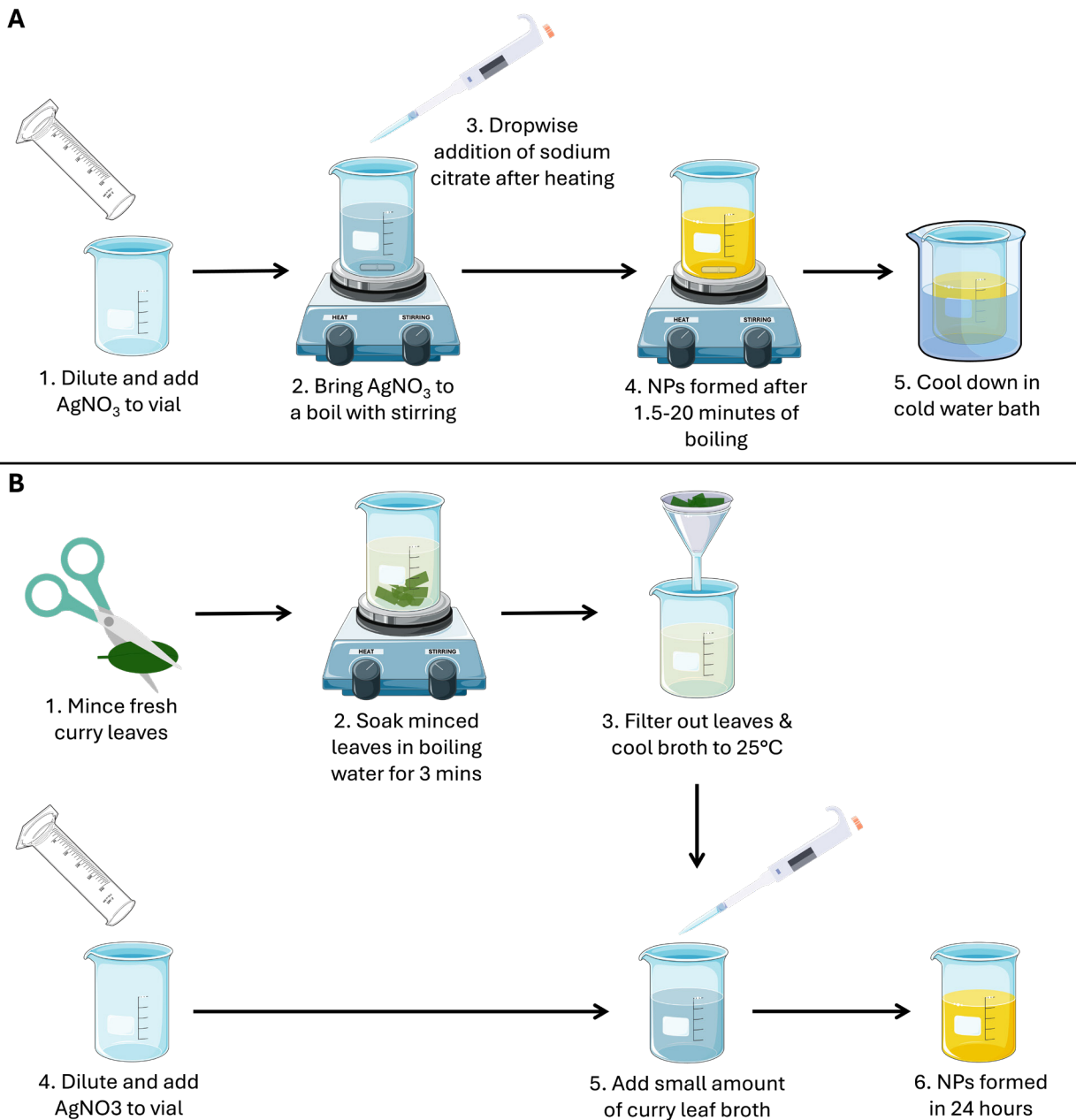


**Figure 5. Synthesis of silver nanoparticles (AgNPs).** The procedure for synthesizing citrate-capped (panel A) and plant-based (panel B) silver nanoparticles. Generated using icons from [bioicons.com](http://bioicons.com).

spectrometer would read absorption values above 1 and produce low-quality, erratic data due to sensor noise at such low light levels. In such cases, the nanoparticles were diluted with distilled water until all absorbance readings came below 1, and the readings could be multiplied by the dilution ratio to get the true absorption values.

#### Phase 2: Exposing Specimens to AgNPs

*E. coli* was chosen as a representative microbe because it is a commonly used model organism that allows this study's results to be compared to data from other studies or interventions (14,21,22). *D. melanogaster* was chosen to represent complex organisms because it is one of the most

well-studied model organisms, providing precedent for its use as a model for humans (36). During this phase of the study, *E. coli* and *D. melanogaster* were exposed to AgNPs of different sizes, concentrations, and surface coatings. The AgNPs' sizes varied between 41 and 85 nm. The concentrations used were 2, 20, and 40 mg/L of silver; citrate and plant-based surface coatings were used.

#### *E. coli* Testing

The first step in *E. coli* testing involved preparing the culture. To prepare this culture, nutrient broth (Carolina Biology, Catalog No. 785360) was inoculated with a Bacto Bead (Edvotek, *E. coli*) (Figure 6A, step 1). The broth was

incubated for 24 hours at 37°C (**Figure 6A**, step 2). The culture was then serially diluted to a 10-3 dilution (**Figure 6A**, step 3). This culture was used within 45 minutes of finishing the incubation. Testing followed the preparation of the culture.

For *E. coli* testing, the spread plate procedure was used with diluted liquid culture mixed with different AgNP solutions (37). Different AgNPs and *E. coli* broth were mixed to form 220 µL solutions, with AgNPs at 2.0 or 20.0 mg/L concentration and *E. coli* at a 10<sup>-4</sup> dilution. The solutions were pipetted into 60 mm LB agar plates (Carolina biology), and the plates were incubated at 37°C for 24 hours (**Figure 6A**, step 5–6). The number of colonies in each plate was recorded for each tested combination of AgNP size, concentration, and coating agent (**Figure 6A**, step 7). Bacterial toxicity was calculated by the reduction in colony growth using the equation  $(x-c)/c$ , where  $c$  is the average number of colonies in the control (water) and  $x$  is the average number of colonies in the AgNP sample.

#### D. melanogaster Testing

The first step in *D. melanogaster* testing involved the preparation of the fruit fly media. Carolina Biology 4-24 medium with blue coloring, baker's yeast, and diluted AgNP solution (either 20 or 40 mg/L; distilled water for control) were mixed into a fruit fly culture tube.

The next step involved adding *D. melanogaster* to the culture tubes prepared in the first step. For this step, flightless fruit flies (Imagitarium by Petco) were placed in a -20°C freezer for seven minutes, which made the flies unconscious before being transferred onto a cold surface, which kept the

flies unconscious while working (**Figure 6B**, step 1–2). Flies were separated into groups of five males and five females (naked eye observation), and each of these groups (ten flies) was transferred to a culture tube (**Figure 6B**, step 3–4). The flies were allowed to lay eggs in the media for seven days.

After seven days, the culture tubes were placed in a -20°C freezer for 30 minutes to kill all larvae/pupae. Then, larvae above 2 mm long and all pupae within the media/tubes were sorted, and the sum of both was recorded as the number of larvae within the data. The number of counted larvae/pupae was used as the measure of a culture's growth.

#### Statistical Analysis

Microsoft Excel was used for the statistical analysis. When analyzing the effect of a single variable (or sometimes two), such as concentration, all data points were grouped according to that specific variable. Other variables—such as particle size—were intentionally ignored during this step to isolate the variable of interest. If the variable being tested had only two categories or levels (e.g., low vs. high concentration, or presence vs. absence of surface coating), independent *t*-tests were conducted to assess whether the differences between the two groups were statistically significant. This approach allowed the evaluation of the impact of one variable. On the other hand, this approach also caused larger-than-expected standard deviations on some graphs, as other variables also changed the toxicity that were not accounted for, but conclusions were still valid and supported by statistical tests. Additionally, for each set

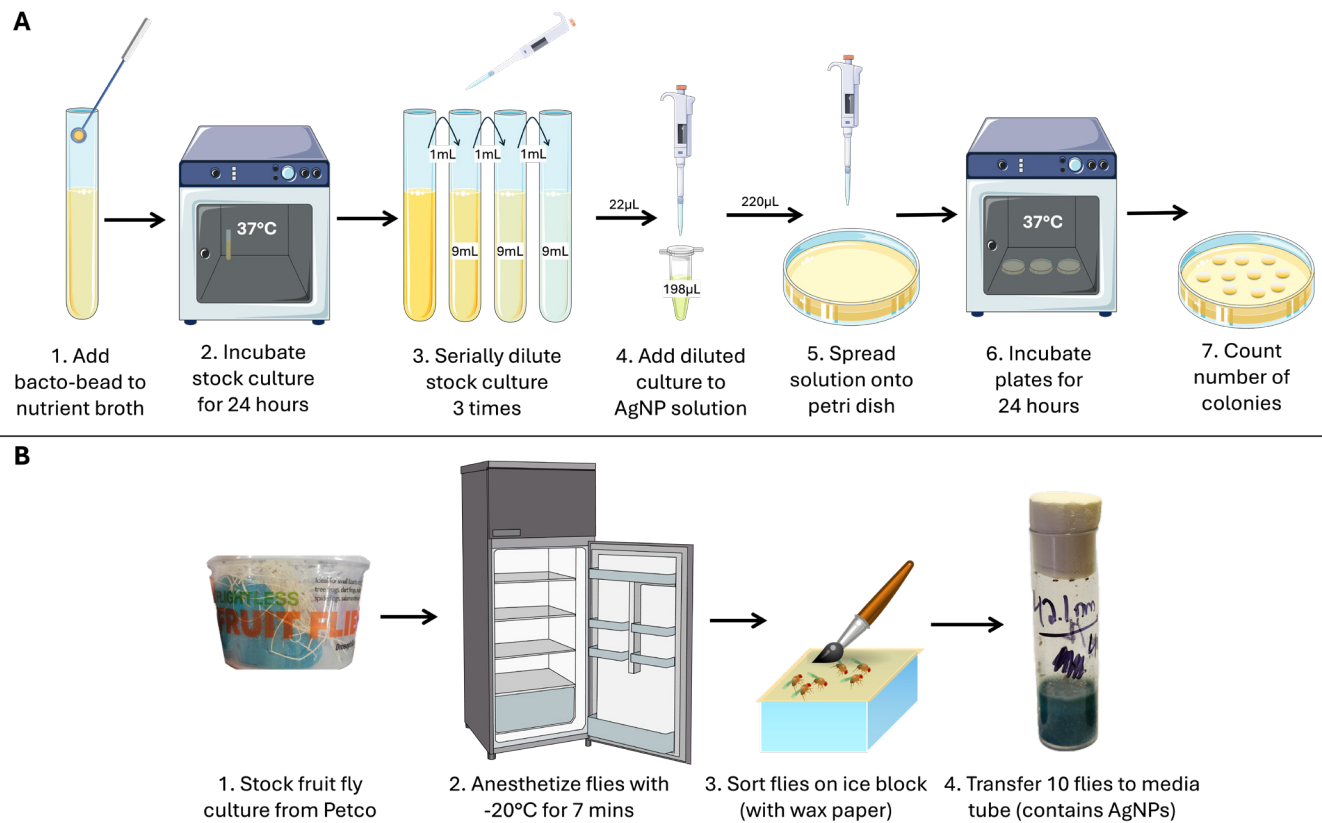


**Figure 6. Workflow for testing the effects of AgNPs on *E. coli* (panel A) and *D. melanogaster* larval growth (panel B).** The procedure used to test the toxicity of AgNPs within both model organisms (icons from [bioicons.com](http://bioicons.com)).

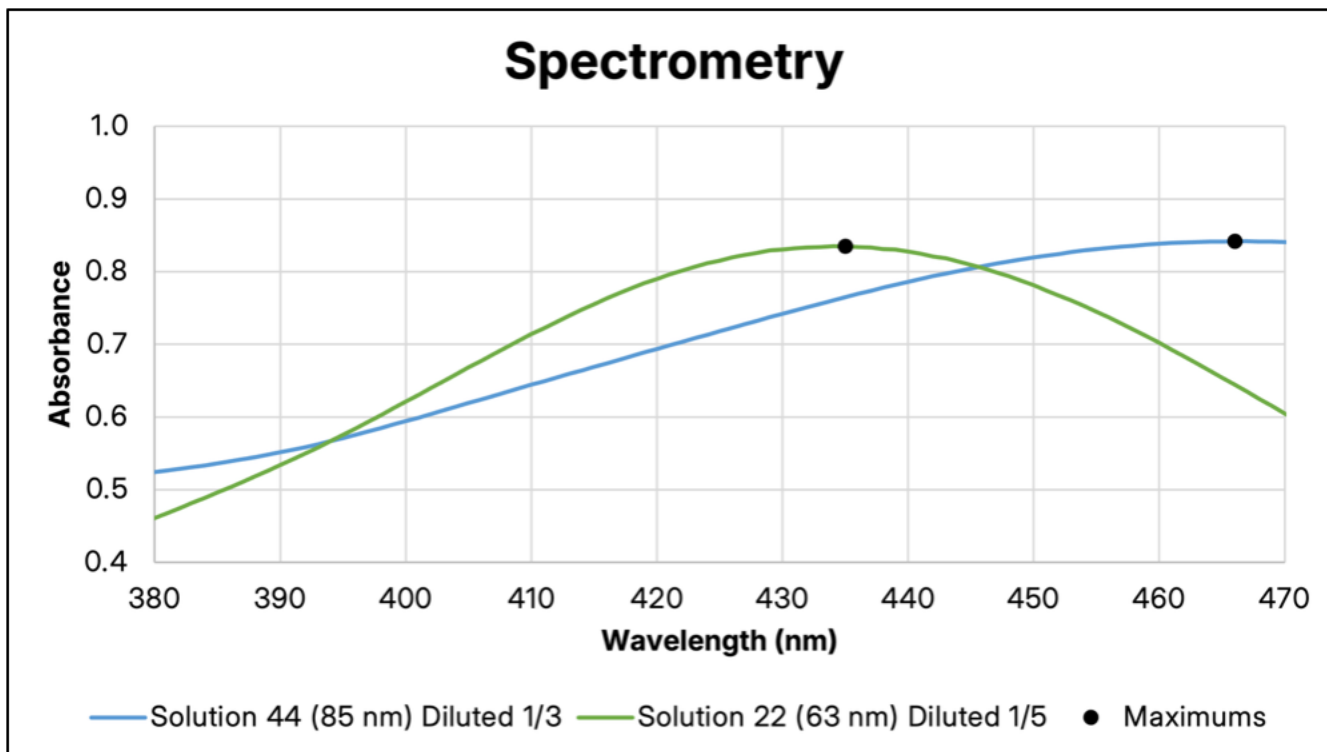


**Figure 7. AgNP absorption spectra.** Spectra shown from two AgNP sample preparations, with absorption on the y-axis and the wavelength on the x-axis. Solution 44 (blue line), large plant-based AgNPs; and solution 22 (green line), medium-sized citrate-capped AgNPs, were measured. Absorption spectra were used to find the size and concentration of AgNPs, as larger AgNPs absorb longer wavelengths.

of data (except for *D. melanogaster* due to low sample sizes), a one-way ANOVA (Analysis of Variance) was conducted on the complete dataset. To further demonstrate significance, a Dunnett's post-hoc test was conducted, as the Dunnett's test compares multiple experimental groups to one control group. The resulting *p*-values determined the placement of asterisks above each bar in the figures, indicating the level of statistical significance. These visual markers help highlight which groups showed statistically significant differences from the control.

#### ACKNOWLEDGMENTS

The authors would like to extend their gratitude to Dr. Bharat Baruah from Kennesaw State University for guiding them on silver nanoparticle synthesis, supplying lab chemicals for synthesis, providing access to a UV-vis spectrophotometer for nanoparticle characterization, and offering support whenever synthesis attempts were unsuccessful. The authors are also thankful to Dr. Link and Mr. Wolfe at Walton High School for providing lab space, equipment, and training that enabled them to conduct the experiments.

**Received:** November 11, 2024

**Accepted:** October 26, 2025

**Published:** XXXX, 2025

#### REFERENCES

1. Barillo, David J., et al. "Silver in medicine: A brief history BC 335 to present." *Burns*, vol. 40, Dec 2014, pp. S3-S8, <https://doi.org/10.1016/j.burns.2014.09.009>.
2. Sim, Wilson, et al. "Antimicrobial Silver in Medicinal and Consumer Applications: A Patent Review of the Past Decade (2007-2017)." *Antibiotics (Basel)*, vol. 7, no. 4, Oct 2018, <https://doi.org/10.3390/antibiotics7040093>.
3. Źyro, Dominik, et al. "Silver, Its Salts and Application in Medicine and Pharmacy." *International Journal of Molecular Sciences*, vol. 24, no. 21, Oct 2023, p. 15723, <https://doi.org/10.3390/ijms242115723>.
4. Alexander, J Wesley. "History of medical use of silver." *Surgical Infections*, vol. 10, no. 3, Jun 2009, pp. 289-292, <https://doi.org/10.1089/sur.2008.9941>.
5. Barras, Frédéric, et al. "Silver and Antibiotic, New Facts to an Old Story." *Antibiotics*, vol. 7, no. 3, Aug 2018, p. 79, <https://doi.org/10.3390/antibiotics7030079>.
6. Yin, I. X., et al. "The Antibacterial Mechanism of Silver Nanoparticles and Its Application in Dentistry." *International Journal of Nanomedicine*, vol. 15, Apr 2020, pp. 2555-2562, <https://doi.org/10.2147/ijn.S246764>.
7. Ali, Zena H., et al. "Efficiency of silver nano particles in removing Escherichia coli ATCC 25922 from drinking water distribution pipes." *Results in Engineering*, vol. 17, Mar 2023, p. 100988, <https://doi.org/10.1016/j.rineng.2023.100988>.
8. Otari, S. V., et al. "Intracellular synthesis of silver nanoparticle by actinobacteria and its antimicrobial activity." *Spectrochim Acta A Mol Biomol Spectrosc*, vol. 136 Pt B, Feb 2015, pp. 1175-1180, <https://doi.org/10.1016/j.saa.2014.10.003>.
9. Xu, L., et al. "Silver nanoparticles: Synthesis, medical applications and biosafety." *Theranostics*, vol. 10, no. 20, Jul 2020, pp. 8996-9031, <https://doi.org/10.7150/thno.45413>.

10. Khan, Muhammad Saleem, *et al.* "Chapter 25 - Toxicity of silver nanoparticles in the aquatic system." *Green Synthesis of Silver Nanomaterials*, Jan 2022, pp. 627-647, <https://doi.org/10.1016/B978-0-12-824508-8.00016-2>.
11. Lu, Wentong, *et al.* "Effect of surface coating on the toxicity of silver nanomaterials on human skin keratinocytes." *Chemical Physics Letters*, vol. 487, no. 1, Feb 2010, pp. 92-96, <https://doi.org/10.1016/j.cplett.2010.01.027>.
12. Simon, Sohail, *et al.* "Biomedical Applications of Plant Extract-Synthesized Silver Nanoparticles." *Biomedicines*, vol. 10, no. 11, Nov 2022, p. 2792.
13. Bamal, Deepak, *et al.* "Silver Nanoparticles Biosynthesis, Characterization, Antimicrobial Activities, Applications, Cytotoxicity and Safety Issues: An Updated Review." *Nanomaterials (Basel)*, vol. 11, no. 8, Aug 2021, <https://doi.org/10.3390/nano11082086>.
14. Qais, Faizan Abyl, *et al.* "Antibacterial Effect of Silver Nanoparticles Synthesized Using *Murraya koenigii* (L.) against Multidrug-Resistant Pathogens." *Bioinorg Chem Appl*, vol. 2019, Jul 2019, p. 4649506, <https://doi.org/10.1155/2019/4649506>.
15. Urnukhsaikhan, Enerelt, *et al.* "Antibacterial activity and characteristics of silver nanoparticles biosynthesized from *Carduus crispus*." *Scientific Reports*, vol. 11, no. 1, Oct 2021, p. 21047, <https://doi.org/10.1038/s41598-021-00520-2>.
16. Park, Margriet V. D. Z., *et al.* "The effect of particle size on the cytotoxicity, inflammation, developmental toxicity and genotoxicity of silver nanoparticles." *Biomaterials*, vol. 32, no. 36, 2011/12/01, pp. 9810-9817, <https://doi.org/https://doi.org/10.1016/j.biomaterials.2011.08.085>.
17. Martin, Megan E., *et al.* "Silver nanoparticles alter epithelial basement membrane integrity, cell adhesion molecule expression, and TGF- $\beta$ 1 secretion." *Nanomedicine: Nanotechnology, Biology and Medicine*, vol. 21, Oct 2019, p. 102070, <https://doi.org/https://doi.org/10.1016/j.nano.2019.102070>.
18. Xiao, Hefang, *et al.* "Silver nanoparticles induce cell death of colon cancer cells through impairing cytoskeleton and membrane nanostructure." *Micron*, vol. 126, Nov 2019, p. 102750, <https://doi.org/https://doi.org/10.1016/j.micron.2019.102750>.
19. Ayala-Núñez, Nilda Vanesa, *et al.* "Silver Nanoparticles Toxicity and Bactericidal Effect Against Methicillin-Resistant *Staphylococcus aureus*: Nanoscale Does Matter." *NanoBiotechnology*, vol. 5, no. 1, Dec 2009, pp. 2-9, <https://doi.org/10.1007/s12030-009-9029-1>.
20. Quinteros, M. A., *et al.* "Oxidative stress generation of silver nanoparticles in three bacterial genera and its relationship with the antimicrobial activity." *Toxicology in Vitro*, vol. 36, Oct 2016, pp. 216-223, <https://doi.org/https://doi.org/10.1016/j.tiv.2016.08.007>.
21. Ivask, A., *et al.* "Toxicity mechanisms in *Escherichia coli* vary for silver nanoparticles and differ from ionic silver." *ACS Nano*, vol. 8, no. 1, Jan 2014, pp. 374-386, <https://doi.org/10.1021/nn4044047>.
22. Sondi, Ivan, *et al.* "Silver nanoparticles as antimicrobial agent: a case study on *E. coli* as a model for Gram-negative bacteria." *J Colloid Interface Sci*, vol. 275, no. 1, Jul 2004, pp. 177-182, <https://doi.org/10.1016/j.jcis.2004.02.012>.
23. Martínez-Castañón, G. A., *et al.* "Synthesis and antibacterial activity of silver nanoparticles with different sizes." *Journal of Nanoparticle Research*, vol. 10, no. 8, Dec 2008, pp. 1343-1348, <https://doi.org/10.1007/s11051-008-9428-6>.
24. Recordati, C., *et al.* "Tissue distribution and acute toxicity of silver after single intravenous administration in mice: nano-specific and size-dependent effects." *Part Fibre Toxicol*, vol. 13, Feb 2016, p. 12, <https://doi.org/10.1186/s12989-016-0124-x>.
25. Kong, I. C., *et al.* "Evaluation of the Effects of Particle Sizes of Silver Nanoparticles on Various Biological Systems." *Int J Mol Sci*, vol. 21, no. 22, Nov 2020, <https://doi.org/10.3390/ijms21228465>.
26. Béltéky P, Rónavári A, Zakupszky D, Boka E, Igaz N, Szerencsés B, Pfeiffer I, Vágvölgyi C, Kiricsi M, Kónya Z. "Are Smaller Nanoparticles Always Better? Understanding the Biological Effect of Size-Dependent Silver Nanoparticle Aggregation Under Biorelevant Conditions." *International Journal of Nanomedicine*, vol. 2021:16, 2023/04/23/, pp. 3021-3040, <https://doi.org/10.2147/IJN.S304138>.
27. Liu, Wei, *et al.* "Impact of silver nanoparticles on human cells: effect of particle size." *Nanotoxicology*, vol. 4, no. 3, Sep, pp. 319-330, <https://doi.org/10.3109/17435390.2010.483745>.
28. Wäng, Yán, *et al.* "Developmental impacts and toxicological hallmarks of silver nanoparticles across diverse biological models." *Environmental Science and Ecotechnology*, vol. 19, May 2024, p. 100325, <https://doi.org/10.1016/j.ese.2023.100325>.
29. Mang'era, Clarence Maikuri, *et al.* "Growth-disrupting *Murraya koenigii* leaf extracts on *Anopheles gambiae* larvae and identification of associated candidate bioactive constituents." *Acta Tropica*, vol. 190, Feb 2019, pp. 304-311, <https://doi.org/10.1016/j.actatropica.2018.12.009>.
30. Yadav, Radha, *et al.* "Comparative assessment of green and chemically synthesized glutathione capped silver nanoparticles for antioxidant, mosquito larvicidal and eco-toxicological activities." edited by vol. 13, *Nature*, May 2023 2023. [doi:10.1038/s41598-023-35249-7](https://doi.org/10.1038/s41598-023-35249-7).
31. Nguyen, Ngoc Phuong Uyen, *et al.* "Synthesis of Silver Nanoparticles: From Conventional to 'Modern' Methods—A Review." *Processes*, vol. 11, no. 9, Sep 2023, p. 2617, <https://doi.org/10.3390/pr11092617>.
32. Iwaji, Chika, *et al.* "Synthesis and characterization of silver nanoparticles and their promising antimicrobial effects." *Chemical Physics Impact*, vol. 9, Dec 2024, p. 100758, <https://doi.org/https://doi.org/10.1016/j.chphi.2024.100758>.
33. Pillai, Zeena S., *et al.* "What Factors Control the Size and Shape of Silver Nanoparticles in the Citrate Ion Reduction Method?" *The Journal of Physical Chemistry B*, vol. 108, no. 3, Jan 2004, pp. 945-951, <https://doi.org/10.1021/jp037018r>.
34. Paramelle, D., *et al.* "A rapid method to estimate the concentration of citrate capped silver nanoparticles from UV-visible light spectra." *Analyst*, vol. 139, no. 19, Jul 2014, pp. 4855-4861, <https://doi.org/10.1039/C4AN00978A>.
35. Wimuktiwan, Panida, *et al.* "Investigation of silver nanoparticles and plasma protein association using flow field-flow fractionation coupled with inductively coupled

plasma mass spectrometry (FIFFF-ICP-MS)." *Journal of Analytical Atomic Spectrometry*, vol. 30, no. 1, Oct 2015, pp. 245-253, <https://doi.org/10.1039/C4JA00225C>.

36. Vecchio, Giuseppe. "A fruit fly in the nanoworld: once again *Drosophila* contributes to environment and human health." *Nanotoxicology*, vol. 9, no. 2, Apr 2014, pp. 135-137, <https://doi.org/10.3109/17435390.2014.911985>.

37. Wise, Kathryn. "Preparing Spread Plates Protocols." *ASM Conference for Undergraduate Educators*, edited by American Society for Microbiology, Oct 2006.

**Copyright:** © 2025 Ghosh and Hendricks. All JEI articles are distributed under the attribution non-commercial, no derivative license (<http://creativecommons.org/licenses/by-nc-nd/4.0/>). This means that anyone is free to share, copy and distribute an unaltered article for non-commercial purposes provided the original author and source is credited.